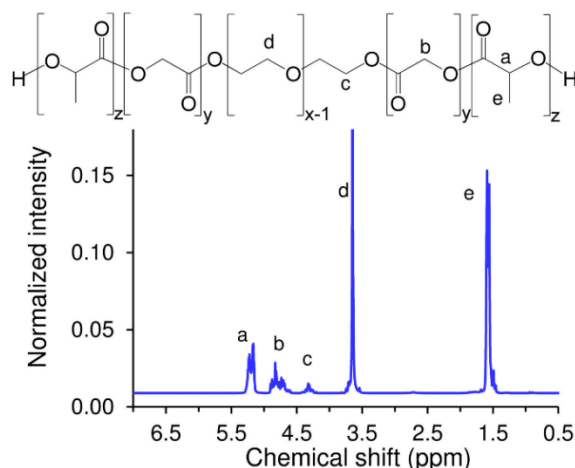




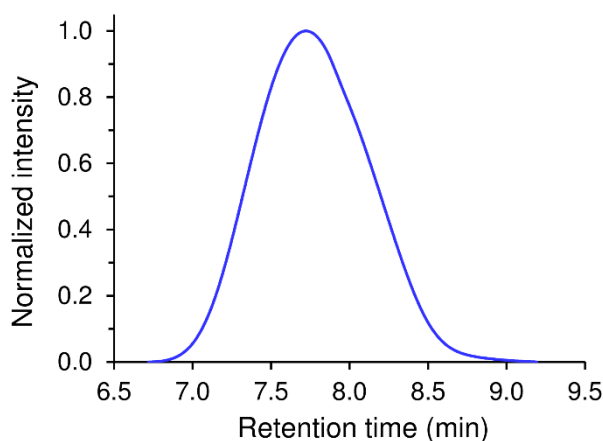
1 *Supplementary materials*

2 **The effect of the thermosensitive biodegradable**
3 **PLGA-PEG-PLGA copolymer on the rheological,**
4 **structural and mechanical properties of thixotropic**
5 **self-hardening tricalcium phosphate cement**



6

7 **Figure S1.** ^1H NMR spectrum of PLGA–PEG–PLGA copolymer. Molecular weight and molar
8 composition of copolymer were determined from integrals of characteristic proton intensities of lactic
9 acid ($\text{O}(\text{CH}_3)\text{CHO}$) in a range between $\delta = 5.1 - 5.35$ ppm (multiplet, 1H) (a) and ($\text{OC}(\text{CH}_3)\text{CHO}$)
10 protons at $\delta = 1.5 - 1.75$ ppm (multiplet, 3H) (e), glycolic acid (OCH_2O) at $\delta = 4.6 - 4.9$ ppm (multiplet,
11 2H) (b), PEG ($\text{OCH}_2\text{CH}_2\text{O}$) at $\delta = 3.55 - 3.75$ ppm (multiplet, 3H) (d). The real molecular weight of the
12 copolymer is $5\,210\text{ g}\cdot\text{mol}^{-1}$, PLGA/PEG weight ratio 2.47 and LA/GA molar ratio 2.96.

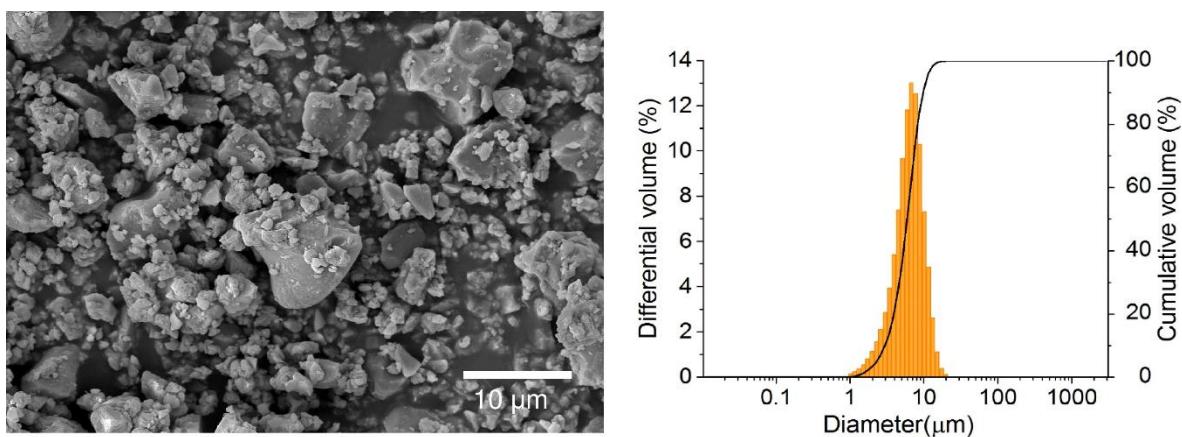


13

14 **Figure S2.** Gel permeation chromatography with the multi-angle light scattering (GPC-MALS) of
15 PLGA-PEG-PLGA copolymer. The measured number-average molecular weight (M_n) and
16 polydispersity index (M_w/M_n) were $5300\text{ g}\cdot\text{mol}^{-1}$ and 1.23, respectively.

17

18

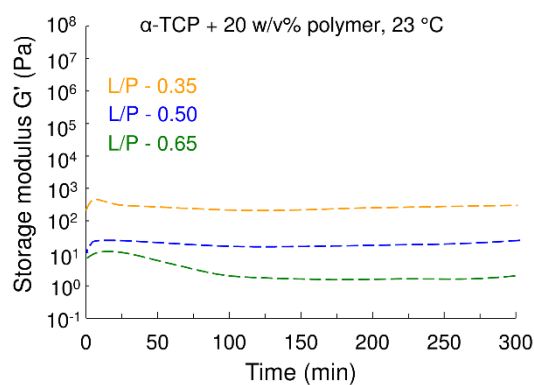


19

(a)

(b)

20 **Figure S3.** Scanning electron micrograph (a) and particle size distribution (b) for α -TCP powder
 21 component of the CPCs.

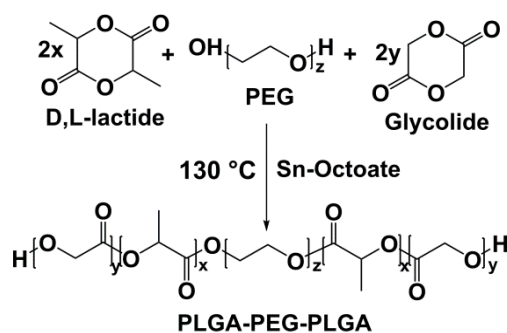


22

23 **Figure S4.** Time-sweep curves of α -TCP cement pastes with different L/P ratio (0.35; 0.5; 0.65 $\text{g}\cdot\text{g}^{-1}$)
 24 and 20 w/v % polymer solution at 23 °C.

25

26



27

28 **Figure S5.** Synthesis of the PLGA—PEG—PLGA triblock copolymer via ring-opening polymerization
 29 technique.